Azimuthally Sensitive Hanbury Brown–Twiss Interferometry in Au + Au Collisions at $\sqrt{s_{NN}} = 200$ GeV

J. Adams,[3] C. Adler,[13] M. M. Aggarwal,[27] Z. Ahammed,[40] J. Amonett,[19] B. D. Anderson,[19] D. Arkhipkin,[12] G. S. Averichev,[11] S. K. Badyal,[18] J. Balewski,[15] O. Barannikova,[30,11] L. S. Barnby,[3] J. Baudot,[17] S. Bekele,[26] V. V. Belaga,[11] R. Bellwied,[43] J. Berger,[13] B. I. Bezverkhny,[45] S. Bhardwaj,[31] A. K. Bhati,[27] H. Bichsel,[42] A. Billmeier,[43] L. C. Bland,[2] C. O. Blyth,[3] B. E. Bonner,[32] M. Botje,[25] A. Boucham,[36] A. Brandin,[23] A. Bravar,[2] R.V. Cadman,[1] X. Z. Cai,[35] H. Caines,[45] M. Calderón de la Barca Sánchez,[2] J. Carroll,[20] J. Castillo,[20] D. Cebra,[5] P. Chaloupka,[10] S. Chattopadhyay,[40] H. F. Chen,[34] Y. Chen,[6] S. P. Chernenko,[11] M. Cherney,[9] A. Chikanian,[45] W. Christie,[2] J. P. Coffin,[17] T. M. Cormier,[43] J. G. Cramer,[42] H. J. Crawford,[4] D. Das,[40] S. Das,[40] A. A. Derevschikov,[29] L. Didenko,[2] T. Dietel,[13] W. J. Dong,[6] X. Dong,[34,20] J. E. Draper,[5] F. Du,[45] A. K. Dubey,[16] V. B. Dunin,[11] J. C. Dunlop,[2] M. R. Dutta Majumdar,[40] V. Eckardt,[21] L. G. Efimov,[11] V. Emelianov,[23] J. Engelage,[4] G. Eppley,[32] B. Erazmus,[36] M. Estienne,[36] P. Fachini,[2] V. Faine,[2] J. Faivre,[17] R. Fatemi,[15] K. Filimonov,[20] P. Filip,[10] E. Finch,[45] Y. Fisyak,[2] D. Flierl,[13] K. J. Foley,[2] J. Fu,[44] C. A. Gagliardi,[37] N. Gagunashvili,[11] J. Gans,[45] M. S. Ganti,[40] L. Gaudichet,[36] F. Geurts,[32] V. Ghazikhanian,[6] P. Ghosh,[40] J. E. Gonzalez,[6] O. Grachov,[43] O. Grebenyuk,[25] S. Gronstal,[9] D. Grosnick,[39] S. M. Guertin,[6] A. Gupta,[18] T. D. Gutierrez,[5] T. J. Hallman,[2] A. Hamed,[43] D. Hardtke,[20] J.W. Harris,[45] M. Heinz,[45] T.W. Henry,[37] S. Heppelmann,[28] B. Hippolyte,[45] A. Hirsch,[30] E. Hjort,[20] G.W. Hoffmann,[38] M. Horsley,[45] H. Z. Huang,[6] S. L. Huang,[34] E. Hughes,[7] T. J. Humanic,[26] G. Igo,[6] A. Ishihara,[38] P. Jacobs,[20] W.W. Jacobs,[15] M. Janik,[41] H. Jiang,[6,20] I. Johnson,[20] P. G. Jones,[3] E. G. Judd,[4] S. Kabana,[45] M. Kaplan,[8] D. Keane,[19] V. Yu. Khodyrev,[29] J. Kiryluk,[6] A. Kisiel,[41] J. Klay,[20] S. R. Klein,[20] A. Klyachko,[15] D. D. Koetke,[39] T. Kollegger,[13] M. Kopytine,[19] L. Kotchenda,[23] A. D. Kovalenko,[11] M. Kramer,[24] P. Kravtsov,[23] V. I. Kravtsov,[29] K. Krueger,[1] C. Kuhn,[17] A. I. Kulikov,[11] A. Kumar,[27] G. J. Kunde,[45] C. L. Kunz,[8] R. Kh. Kutuev,[12] A. A. Kuznetsov,[11] M. A. C. Lamont,[3] J. M. Landgraf,[2] S. Lange,[13] B. Lasiuk,[45] F. Laue,[2] J. Lauret,[2] A. Lebedev,[2] R. Lednický,[11] M. J. LeVine,[2] C. Li,[34] Q. Li,[43] S. J. Lindenbaum,[24] M. A. Lisa,[26] F. Liu,[44] L. Liu,[44] Z. Liu,[44] Q. J. Liu,[42] T. Ljubicic,[2] W. J. Llope,[32] H. Long,[6] R. S. Longacre,[2] M. Lopez-Noriega,[26] W. A. Love,[2] T. Ludlam,[2] D. Lynn,[2] J. Ma,[6] Y. G. Ma,[35] D. Magestro,[26] S. Mahajan,[18] L. K. Mangotra,[18] D. P. Mahapatra,[16] R. Majka,[45] R. Manweiler,[39] S. Margetis,[19] C. Markert,[45] L. Martin,[36] J. Marx,[20] H. S. Matis,[20] Yu. A. Matulenko,[29] C. J. McClain,[1] T. S. McShane,[9] F. Meissner,[20] Yu. Melnick,[29] A. Meschanin,[29] M. L. Miller,[45] Z. Milosevich,[8] N. G. Minaev,[29] C. Mironov,[19] A. Mischke,[25] D. Mishra,[16] J. Mitchell,[32] B. Mohanty,[40] L. Molnar,[30] C. F. Moore,[38] M. J. Mora-Corral,[21] D. A. Morozov,[29] V. Morozov,[20] M. M. de Moura,[33] M. G. Munhoz,[33] B. K. Nandi,[40] S. K. Nayak,[18] T. K. Nayak,[40] J. M. Nelson,[3] P. K. Netrakanti,[40] V. A. Nikitin,[12] L.V. Nogach,[29] B. Norman,[19] S. B. Nurushev,[29] G. Odyniec,[20] A. Ogawa,[2] V. Okorokov,[23] M. Oldenburg,[20] D. Olson,[20] G. Paic,[26] S. K. Pal,[40] Y. Panebratsev,[11] S. Y. Panitkin,[2] A. I. Pavlinov,[43] T. Pawlak,[41] T. Peitzmann,[25] V. Perevoztchikov,[2] C. Perkins,[4] W. Peryt,[41] V. A. Petrov,[12] S. C. Phatak,[16] R. Picha,[5] M. Planinic,[46] J. Pluta,[41] N. Porile,[30] J. Porter,[2] A. M. Poskanzer,[20] M. Potekhin,[2] E. Potrebenikova,[11] B.V. K. S. Potukuchi,[18] D. Prindle,[42] C. Pruneau,[43] J. Putschke,[21] G. Rai,[20] G. Rakness,[15] R. Raniwala,[31] S. Raniwala,[31] O. Ravel,[36] R. L. Ray,[38] S.V. Razin,[11,15] D. Reichhold,[30] J. G. Reid,[42] J. G. Reid,[42] G. Renault,[36] F. Retiere,[20] A. Ridiger,[23] H. G. Ritter,[20] J. B. Roberts,[32] O.V. Rogachevski,[11] J. L. Romero,[5] A. Rose,[43] C. Roy,[36] L. J. Ruan,[34,2] R. Sahoo,[16] I. Sakrejda,[20] S. Salur,[45] J. Sandweiss,[45] I. Savin,[12] J. Schambach,[38] R. P. Scharenberg,[30] N. Schmitz,[21] L. S. Schroeder,[20] K. Schweda,[20] J. Seger,[9] P. Seyboth,[21] E. Shahaliev,[11] M. Shao,[34] W. Shao,[7] M. Sharma,[27] K. E. Shestermanov,[29] S. S. Shimanskii,[11] R. N. Singaraju,[40] F. Simon,[21] G. Skoro,[11] N. Smirnov,[45] R. Snellings,[25] G. Sood,[27] P. Sorensen,[20] J. Sowinski,[15] J. Speltz,[17] H. M. Spinka,[1] B. Srivastava,[30] T. D. S. Stanislaus,[39] R. Stock,[13] A. Stolpovsky,[43] M. Strikhanov,[23] B. Stringfellow,[30] C. Struck,[13] A. A. P. Suaide,[33] E. Sugarbaker,[26] C. Suire,[2] M. Šumbera,[10] B. Surrow,[2] T. J. M. Symons,[20] A. Szanto de Toledo,[33] P. Szarwas,[41] A. Tai,[6] J. Takahashi,[33] A. H. Tang,[2,25] D. Thein,[6] J. H. Thomas,[20] S. Timoshenko,[23] M. Tokarev,[11] M. B. Tonjes,[22] T. A. Trainor,[42] S. Trentalange,[6] R. E. Tribble,[37] O. Tsai,[6] T. Ullrich,[2] D. G. Underwood,[1] G. Van Buren,[2] A. M. VanderMolen,[22] R. Varma,[14] I. Vasilevski,[12] A. N. Vasiliev,[29] R. Vernet,[17] S. E. Vigdor,[15] Y. P. Viyogi,[40] S. A. Voloshin,[43] M. Vznuzdaev,[23] W. Waggoner,[9] F. Wang,[30] G. Wang,[7] G. Wang,[19] X. L. Wang,[34] Y. Wang,[38] Z. M. Wang,[34] H. Ward,[38] J.W. Watson,[19] J. C. Webb,[15] R. Wells,[26] G. D. Westfall,[22] C. Whitten, Jr.,[6] H. Wieman,[20] R. Willson,[26] S.W. Wissink,[15] R. Witt,[45] J. Wood,[6] J. Wu,[34] N. Xu,[20] Z. Xu,[2] Z. Z. Xu,[34] E. Yamamoto,[20] P. Yepes,[32] V. I. Yurevich,[11] B. Yuting,[25] Y.V. Zanevski,[11] H. Zhang,[45,2] W. M. Zhang,[19] Z. P. Zhang,[34] Z. P. Zhaomin,[34] Z. P. Zizong,[34] P. A. Żołnierczuk,[15] R. Zoulkarneev,[12] J. Zoulkarneeva,[12] and A. N. Zubarev[11]

(STAR Collaboration)

[1]Argonne National Laboratory, Argonne, Illinois 60439, USA
[2]Brookhaven National Laboratory, Upton, New York 11973, USA
[3]University of Birmingham, Birmingham, United Kingdom
[4]University of California, Berkeley, California 94720, USA
[5]University of California, Davis, California 95616, USA
[6]University of California, Los Angeles, California 90095, USA
[7]California Institute of Technology, Pasadena, California 91125, USA
[8]Carnegie Mellon University, Pittsburgh, Pennsylvania 15213, USA
[9]Creighton University, Omaha, Nebraska 68178, USA
[10]Nuclear Physics Institute AS CR, Řež/Prague, Czech Republic
[11]Laboratory for High Energy (JINR), Dubna, Russia
[12]Particle Physics Laboratory (JINR), Dubna, Russia
[13]University of Frankfurt, Frankfurt, Germany
[14]Indian Institute of Technology, Mumbai, India
[15]Indiana University, Bloomington, Indiana 47408, USA
[16]Institute of Physics, Bhubaneswar 751005, India
[17]Institut de Recherches Subatomiques, Strasbourg, France
[18]University of Jammu, Jammu 180001, India
[19]Kent State University, Kent, Ohio 44242, USA
[20]Lawrence Berkeley National Laboratory, Berkeley, California 94720, USA
[21]Max-Planck-Institut für Physik, Munich, Germany
[22]Michigan State University, East Lansing, Michigan 48824, USA
[23]Moscow Engineering Physics Institute, Moscow Russia
[24]City College of New York, New York City, New York 10031, USA
[25]NIKHEF, Amsterdam, The Netherlands
[26]The Ohio State University, Columbus, Ohio 43210, USA
[27]Panjab University, Chandigarh 160014, India
[28]Pennsylvania State University, University Park, Pennsylvania 16802, USA
[29]Institute of High Energy Physics, Protvino, Russia
[30]Purdue University, West Lafayette, Indiana 47907, USA
[31]University of Rajasthan, Jaipur 302004, India
[32]Rice University, Houston, Texas 77251, USA
[33]Universidade de Sao Paulo, Sao Paulo, Brazil
[34]University of Science & Technology of China, Anhui 230027, China
[35]Shanghai Institute of Nuclear Research, Shanghai 201800, People's Republic of China
[36]SUBATECH, Nantes, France
[37]Texas A&M University, College Station, Texas 77843, USA
[38]University of Texas, Austin, Texas 78712, USA
[39]Valparaiso University, Valparaiso, Indiana 46383, USA
[40]Variable Energy Cyclotron Centre, Kolkata 700064, India
[41]Warsaw University of Technology, Warsaw, Poland
[42]University of Washington, Seattle, Washington 98195, USA
[43]Wayne State University, Detroit, Michigan 48201, USA
[44]Institute of Particle Physics, CCNU (HZNU), Wuhan, 430079 China
[45]Yale University, New Haven, Connecticut 06520, USA
[46]University of Zagreb, Zagreb, HR-10002, Croatia

We present the results of a systematic study of the shape of the pion distribution in coordinate space at freeze-out in Au + Au collisions at BNL RHIC using two-pion Hanbury Brown–Twiss (HBT) interferometry. Oscillations of the extracted HBT radii versus emission angle indicate sources elongated perpendicular to the reaction plane. The results indicate that the pressure and expansion time of the collision system are not sufficient to completely quench its initial shape.

Relativistic heavy ion collisions are believed to reach sufficiently high energy densities and temperatures for the possible formation of a quark-gluon plasma (QGP) [1]. Hanbury Brown–Twiss (HBT) interferometry [2] of two particle Bose-Einstein correlations directly accesses the space-time structure of the emitting source formed in these collisions, providing crucial probes of the system dynamics. At the BNL Relativistic Heavy Ion Collider (RHIC), identical-pion HBT studies in Au + Au collisions at $\sqrt{s_{NN}} = 130$ GeV [3,4] yielded an apparent

source size consistent with measurements at lower energies, in contrast to predictions of larger sources based on QGP formation [5]. In addition, hydrodynamical models, successful at RHIC in describing transverse momentum spectra and elliptic flow [6], have failed to reproduce the small HBT radii [7]. This so-called "HBT puzzle" [8,9] might arise because the system's lifetime is shorter than predicted by models.

In noncentral collisions, azimuthally sensitive HBT measurements performed relative to the reaction plane provide a measure of the source shape at freeze-out [10–12]. In such collisions, the almond-shaped collision geometry generates greater transverse pressure gradients in the reaction plane than perpendicular to it. This leads to stronger *in-plane* expansion (elliptic flow) [6,13–15] which diminishes the initial *out-of-plane* spatial anisotropy. Therefore the freeze-out source shape should be sensitive to the evolution of the pressure gradients and the system lifetime; a long-lived system would be less out of plane extended and perhaps in plane extended. Hydrodynamic calculations [16] predict a strong sensitivity of the HBT parameters to the early conditions in the collision system and show that, while the system may still be out of plane extended after hydrodynamic evolution, a subsequent rescattering phase [17] tends to make the final source in plane. Knowledge of the freeze-out source shape might discriminate among scenarios of the system's evolution.

In this Letter, we present results of a systematic study of azimuthally sensitive HBT in Au + Au collisions at $\sqrt{s_{NN}} = 200$ GeV. These results allow for first studies of the relationship between the initial and final eccentricities of the system.

The measurements were made using the STAR detector [18] at RHIC. Particle trajectories and momenta were reconstructed using a time projection chamber (TPC) with full azimuthal coverage, located inside a 0.5 T solenoidal magnet. Au + Au events with primary vertices ≤ 25 cm longitudinally of the TPC center were placed into centrality classes following Ref. [19]. A high-multiplicity triggered data set of 5×10^5 events was used for the most-central bin (0%–5% total cross section), and a minimum-bias data set of 1.6×10^6 events was used for all other centrality classes (5%–10%, 10%–20%, 20%–30%, and 30%–80%). The 2nd-order event plane angle Ψ_2 [20] for each event was determined from the weighted sum of primary charged-particle transverse momenta [21]. Within a resolution which we determine from the random subevent method [20], $\Psi_2 \approx \Psi_{rp}$ (true reaction plane angle) or $\Psi_2 \approx \Psi_{rp} + \pi$; i.e., the direction of the impact parameter vector is determined up to a sign [20,22].

Pion candidates, selected according to their specific energy loss (dE/dx) in the TPC in the rapidity range $|y| < 0.5$, were required to pass within 3 cm of the primary vertex and contain > 15 (out of 45) TPC space points in the reconstructed trajectory. Pion pairs were subjected to two requirements. To account for reconstructing a single particle trajectory as two tracks, a topological cut is applied in which a minimum fraction of TPC pad layers must show distinct hits for both tracks. To reduce the effect of merging two particle trajectories into a single reconstructed track, an additional topological cut requires that the number of *merged* TPC hits falls below a maximum fraction. The latter cut leads to a systematic error that depends on the event multiplicity and the transverse momentum of the tracks [3].

Pairs of like-sign pions were placed into bins of $\Phi' \equiv \phi_{pair} - \Psi_2$, where ϕ_{pair} is the azimuthal angle of the pair momentum [$\mathbf{k} = \frac{1}{2}(\mathbf{p}_1 + \mathbf{p}_2)$]. Because we use the 2nd-order reaction plane, Φ' is only defined in the range $(0, \pi)$. For each bin, a three-dimensional correlation function is constructed in the Pratt-Bertsch "out-side-long" decomposition [23] of the relative pair momentum $\mathbf{q}$. The numerator of the correlation function contains pairs of pions from the same event, and the denominator contains pairs of pions from different events which have similar primary vertex position, reaction plane orientation, multiplicity, and magnetic field orientation. π^- pairs and π^+ pairs were mixed separately due to charge-dependent acceptances but are combined to increase statistics; separate π^+ and π^- analyses showed no significant differences.

Finite reaction plane resolution and finite width of the Φ' bins reduce the measured oscillation amplitudes of HBT radii vs Φ'. A model-independent correction procedure [24], applied to each $\mathbf{q}$ bin in the numerator and denominator of each correlation function, accounts for these effects and increases the amplitudes of the HBT radii vs Φ ($\Phi \equiv \phi_{pair} - \Psi_{rp}$). The increase is roughly inversely proportional to the measured [20,21] reaction plane resolution, i.e., the amplitudes increase $\sim 10\%$–30%. All data were corrected using this procedure. Also, autocorrelation contributions to Φ were tested by selecting distinct sets of particles for event plane determination and HBT analysis, with no observed effect.

In addition, correlations due to final-state Coulomb repulsion must be accounted for, in order to isolate the Bose-Einstein correlations of interest. Traditionally this was accomplished by applying correction weights [determined by calculating the Coulomb correlation function $K(\mathbf{q})$ for a spherical Gaussian source [3]] to all pairs in the denominator. Recently, the CERES Collaboration [25] noted that this approach overcorrects for the Coulomb effect and advocated an improved procedure [26] which applies the Coulomb weight only to the fraction of pairs that participate in the Bose-Einstein correlation. We adopt this approach and fit each experimental correlation function to the form:

$$C(\mathbf{q}, \Phi) = N \cdot [(1 - \lambda) \cdot 1 + \lambda \cdot K(\mathbf{q})(1 + G(\mathbf{q}, \Phi))],$$

$$(1)$$

where the $(1 - \lambda)$ and λ terms account for the nonparticipating and participating fractions of pairs, respectively, N is a normalization parameter, and $G(\mathbf{q}, \Phi)$ is the Gaussian correlation model [23]:

$$G(\mathbf{q}, \Phi) = e^{-q_o^2 R_o^2(\Phi) - q_s^2 R_s^2(\Phi) - q_l^2 R_l^2(\Phi) - q_o q_s R_{os}^2(\Phi)}. \quad (2)$$

R_i^2 are the squared HBT radii, where the l, s, and o subscripts indicate the long (parallel to beam), side (perpendicular to beam and total pair momentum), and out (perpendicular to q_l and q_s) decomposition of $\mathbf{q}$ with an additional cross term [27]. Fitting with Eq. (1) caused R_o to increase 10%–20% compared to Coulomb correcting all pairs, while R_s and R_l, respectively, are consistent within errors.

Figure 1 shows the squared HBT radii, obtained using Eq. (1), as a function of Φ for three centrality classes. All pairs with pair transverse momentum $0.15 \leq k_T \leq 0.6 \, \text{GeV}/c$ are included, and each centrality is divided into 12 Φ bins of 15° width. The data point at $\Phi = \pi$ is the reflected $\Phi = 0$ value, and solid lines indicate Fourier expansions of the allowed oscillations [24]:

$$R_{\mu,n}^2(k_T) = \begin{cases} \langle R_\mu^2(k_T, \Phi) \cos(n\Phi) \rangle & (\mu = o, s, l), \\ \langle R_\mu^2(k_T, \Phi) \sin(n\Phi) \rangle & (\mu = os). \end{cases} \quad (3)$$

As expected [3], the 0th-order Fourier coefficient (FC) indicates larger apparent source sizes for more central collisions. We verified that the 0th-order FC corresponds to the HBT radii from an azimuthally integrated analysis.

Strong 2nd-order oscillations are observed for R_o^2, R_s^2, and R_{os}^2, and the signs of the oscillations are qualitatively self-consistent [10,24], though the amplitude for most-central events is small. Similar oscillations were observed

in a statistics-limited analysis of minimum-bias Au + Au collisions at $\sqrt{s_{NN}} = 130 \, \text{GeV}$ [28]. These oscillations correspond to a pion source spatially extended perpendicular to the reaction plane, as discussed below. The next terms (4th order) in the Fourier expansions [Eq. (3)] are consistent with zero within statistical errors.

The k_T dependence of the oscillations of the HBT radii may contain important information on the initial conditions and equation of state of the system [29]. Figure 2 shows the Φ dependence of HBT radii for midcentral (20%–30%) events for four k_T bins. Because of the additional division of pairs in k_T, only four bins in Φ are used. The 0th-order FC increases with decreasing k_T, which was observed for azimuthally integrated HBT analyses at $\sqrt{s_{NN}} = 130 \, \text{GeV}$ [3] and attributed to pion emission from an expanding source. Strong out-of-plane oscillations are observed for all transverse radii in each k_T bin.

The full results are summarized in Fig. 3, which shows the centrality dependence of the Fourier coefficients for three ranges of k_T. The number of participants for each centrality was determined using a simple nuclear overlap model [19]. Systematic variations of the HBT radii arise due to their sensitivity to the antimerging cut threshold and uncertainty associated with the Coulomb procedure [3]. The total variation is largest for $R_{o,0}^2$ (~10%). The systematic variation on the relative amplitudes plotted in the right panels of Fig. 3 are negligible compared to statistical errors. Also, all correlation functions composing Fig. 3 are corrected for momentum resolution following our prescription in Ref. [3].
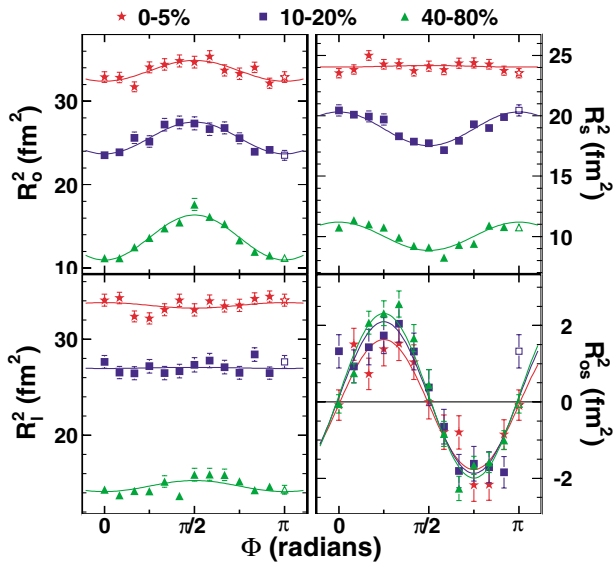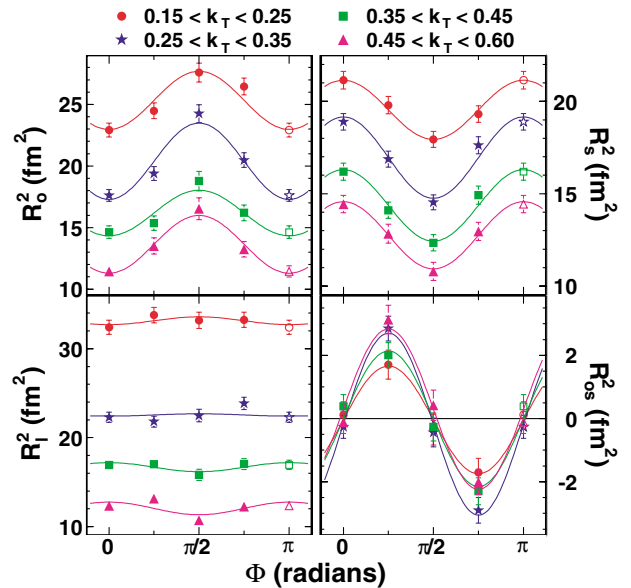

FIG. 1 (color online). Squared HBT radii using Eq. (1) relative to the reaction plane angle for three centrality classes. The solid lines show allowed [24] fits to the individual oscillations.

FIG. 2 (color online). Squared HBT radii relative to the reaction plane angle for four k_T (GeV/c) bins, 20%–30% centrality events. The solid lines show allowed [24] fits to the individual oscillations.
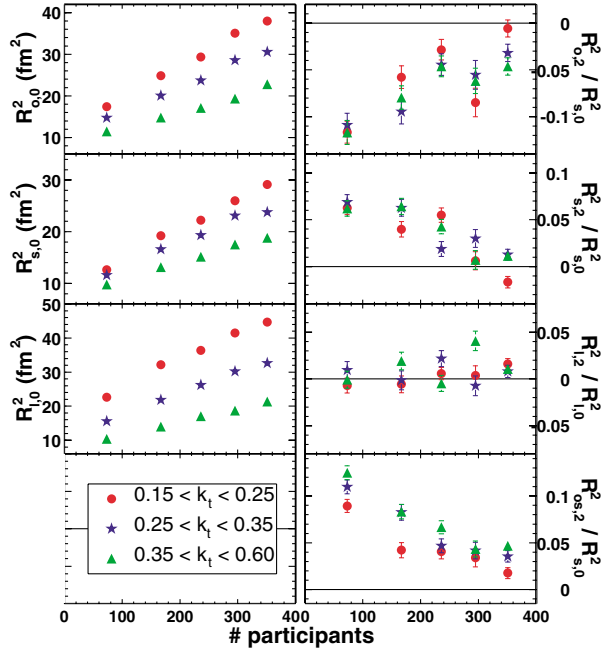
FIG. 3 (color online). Fourier coefficients of azimuthal oscillations of HBT radii vs number of participating nucleons, for three k_T (GeV/c) bins. Left panels: means (0th-order FC) of oscillations; right panels: relative amplitudes (see text for details). Larger participant numbers correspond to more central collisions.

As in Figs. 1 and 2, the 0th-order FCs (left panels) correspond to the squared HBT radii that would be obtained in a standard analysis. $R_{o,0}^2$, $R_{s,0}^2$, and $R_{l,0}^2$ are all observed to decrease for more peripheral collisions. R_o/R_s, found in theoretical calculations to be sensitive to the emission duration of the system [5], is observed to be $R_{o,0}/R_{s,0} = 1.15 \pm 0.01$ (1.06 ± 0.01) for the lowest (highest) k_T bin for 0%–5% most-central events. These values are consistent with that reported at $\sqrt{s_{NN}} = 130$ GeV [3] when the increase in R_o due to the improved Coulomb correction [Eq. (1)] is accounted for. R_o/R_s is still smaller than the predictions from hydrodynamical models, indicating the HBT puzzle persists at $\sqrt{s_{NN}} = 200$ GeV.

Dynamical effects on the homogeneity region affect $R_{\mu,2}^2(k_T)$ as well as $R_{\mu,0}^2$ [16,30]. The *relative* amplitudes of the oscillations offer a more robust measure of the spatial anisotropy and are less sensitive to dynamical effects [30]. Figure 3 shows (right panels) the relative amplitudes vs number of participants for three k_T ranges, using the ratios $R_{\alpha,2}^2/R_{s,0}^2$ ($\alpha = o, s, os$) and $R_{l,2}^2/R_{l,0}^2$. The relative amplitudes for all three transverse radii decrease in magnitude with increasing number of participants, and their weak k_T dependence agrees qualitatively with hydrodynamical calculations [16].

To extract the shape of the pion source at freeze-out, a model-dependent approach is required. In the presence of collective flow the HBT radii correspond to regions of homogeneity [31] and do not reflect the entire source. The "blast-wave" parametrization [6,30,32,33] of freeze-out, which incorporates both spatial and dynamical anisotropies, has been used to describe various observables at $\sqrt{s_{NN}} = 130$ GeV [30,34]. A recent blast-wave analysis [30] showed that the relative oscillation amplitudes (e.g., shown in Fig. 3) are most sensitive to the spatial anisotropy. The source eccentricity $[\varepsilon \equiv (R_y^2 - R_x^2)/(R_y^2 + R_x^2)]$ can be related to the relative amplitude of the HBT oscillations by $\varepsilon_{final} \approx 2R_{s,2}^2/R_{s,0}^2$ [10,30], where R_x (R_y) is the radius of the elliptical source in plane (out of plane).

The eccentricity of the initial almond-shaped overlap region was calculated from a Glauber model [19] using the rms values for R_y and R_x. Figure 4 shows the relation between the initial and final eccentricities obtained by averaging the three k_T bins in Fig. 3. The initial and final eccentricities exhibit a monotonic relationship, with more peripheral collisions showing a larger final anisotropy. Within this model-dependent picture, the source at freeze-out still retains some of its initial shape, indicating that the outward pressure and/or expansion time was not sufficient to quench the initial spatial anisotropy. The large elliptic flow and small HBT radii observed at RHIC energies might favor a large pressure buildup in a short-lived system. Also, out-of-plane freeze-out shapes tend to disfavor a long-lived hadronic rescattering phase following hydrodynamic expansion [17].

In conclusion, we have performed an analysis of two-pion HBT interferometry relative to the reaction plane in Au + Au collisions at $\sqrt{s_{NN}} = 200$ GeV. The relative amplitudes of the HBT radius oscillation are largest for peripheral collisions, indicating larger out-of-plane anisotropy in the pion source at freeze-out, for collisions with larger initial spatial anisotropy. No strong k_T dependence of the relative oscillation amplitudes is observed. The out-of-plane freeze-out shape of the source indicates that the buildup of pressure and the evolution time of the
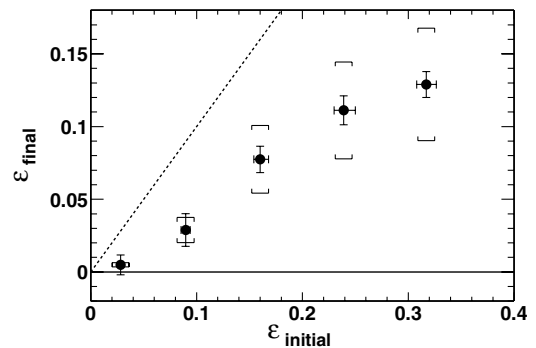

FIG. 4. Source eccentricity obtained with azimuthally sensitive HBT (ε_{final}) vs initial eccentricity from a Glauber model ($\varepsilon_{initial}$). The most peripheral collisions correspond to the largest eccentricity. The dashed line indicates $\varepsilon_{initial} = \varepsilon_{final}$. Uncertainties on the precise nature of space-momentum correlations lead to 30% systematic errors on ε_{final} [30].

expanding system are not sufficient to quench the initial geometry of the collision. This information, taken together with the size of the source and anisotropies in momentum space, places significant constraints on future theoretical efforts to describe the nature and time scale of the collision's evolution.

---

[1] For reviews and recent developments, see Nucl. Phys. **A715**, 1c (2003).
[2] U. Heinz and B.V. Jacak, Annu. Rev. Nucl. Part. Sci. **49**, 529 (1999).
[3] C. Adler et al., Phys. Rev. Lett. **87**, 082301 (2001).
[4] K. Adcox et al., Phys. Rev. Lett. **88**, 242301 (2002).
[5] D. H. Rischke and M. Gyulassy, Nucl. Phys. **A608**, 479 (1996); D. H. Rischke, Nucl. Phys. **A610**, 88c (1996).
[6] C. Adler et al., Phys. Rev. Lett. **87**, 182301 (2001).
[7] U.W. Heinz and P. F. Kolb, Nucl. Phys. **A702**, 269 (2002).
[8] U. Heinz, Nucl. Phys. **A721**, 30 (2003).
[9] A. Dumitru, nucl-th/0206011.
[10] U. A. Wiedemann and U. Heinz, Phys. Rep. **319**, 145 (1999); U. A. Wiedemann, Phys. Rev. C **57**, 266 (1998).
[11] M. A. Lisa et al., Phys. Lett. B **496**, 1 (2000).
[12] S. A. Voloshin and W. E. Cleland, Phys. Rev. C **53**, 896 (1996).
[13] P. F. Kolb, J. Sollfrank, and U. Heinz, Phys. Rev. C **62**, 054909 (2000).
[14] S. A. Voloshin, Nucl. Phys. **A715**, 379c (2003).
[15] J. Y. Ollitrault, nucl-ex/9711003.
[16] P. F. Kolb and U. Heinz, Nucl. Phys. **A715**, 653 (2003).
[17] D. Teaney, J. Lauret, and E. Shuryak, nucl-th/0110037.
[18] K. H. Ackermann et al., Nucl. Instrum. Methods Phys. Res., Sect. A **499**, 624 (2003).
[19] J. Adams et al., nucl-ex/0311017.
[20] A. M. Poskanzer and S. A. Voloshin, Phys. Rev. C **58**, 1671 (1998).
[21] K. Ackermann, et al., Phys. Rev. Lett. **86**, 402 (2001).
[22] J. Adams et al., Phys. Rev. Lett. **92**, 062301 (2004).
[23] S. Pratt, T. Csörgö, and J. Zimanyi, Phys. Rev. C **42**, 2646 (1990); G. Bertsch, M. Gong, and M. Tohyama, Phys. Rev. C **37**, 1896 (1988).
[24] U. Heinz, A. Hummel, M. A. Lisa, and U. A. Wiedemann, Phys. Rev. C **66**, 044903 (2002).
[25] D. Adamova et al., Nucl. Phys. **A714**, 124 (2003).
[26] M. G. Bowler, Phys. Lett. B **270**, 69 (1991); Yu. M. Sinyukov et al., Phys. Lett. B **432**, 248 (1998).
[27] The general form of Eq. (2) contains cross terms R^2_{ol} and R^2_{sl}; however, without knowledge of the 1st-order reaction plane, these terms vanish by symmetry considerations [24]. R^2_{os} is related to the tilt angle between the emission direction and "out" direction in the Pratt-Bertsch decomposition of relative pair momentum [29].
[28] R. C. Wells, Ph.D. thesis, The Ohio State University, 2002.
[29] U.W. Heinz and P. F. Kolb, Phys. Lett. B **542**, 216 (2002).
[30] F. Retiere and M. A. Lisa, nucl-th/0312024.
[31] Yu. M. Sinyukov, Nucl. Phys. **A566**, 589c (1994).
[32] E. Schnedermann, J. Sollfrank, and U. Heinz, Phys. Rev. C **48**, 2462 (1993).
[33] P. Huovinen et al., Phys. Lett. B **503**, 58 (2001).
[34] J. Adams et al., Phys. Rev. Lett. **91**, 262302 (2003).